JOURNAL OF MATERIALS SCIENCE 12 (1977) 563–576

The development of strength in reaction sintered silicon nitride

B. F. JONES, K. C. PITMAN, M. W. LINDLEY
Admiralty Materials Laboratory, Holton Heath, Poole, Dorset, UK

The development of strength in reaction sintered silicon nitride has been investigated by determining the elastic moduli, fracture mechanics parameters, strengths and critical defect sizes of silicon compacts reacted to various degrees of conversion using "static" or "flowing" nitrogen. The relationship between each property and the nitrided density is shown to be independent of the green silicon compact density but is influenced by the nitriding conditions employed. Young's moduli, rigidity moduli and strengths vary linearly with the nitrided density. After an initial period when increases may occur, the critical defect sizes in both "static" and "flow" materials decrease continuously with increasing nitrided density, although at any particular density they are larger in material produced under "flow" conditions. A model is suggested for the development of the structure of reaction sintered silicon nitride involving the development of a continuous silicon nitride network within the pore space of the original silicon compact. The experimental data are discussed in terms of the proportion of silicon nitride which contributes effectively to the continuous network.

1. Introduction

A knowledge of the size of the critical defects in any material is of importance to both the engineering application of the material and the fundamental understanding of the factors which control its strength. Although a number of suggestions have been made concerning the nature of the critical defects controlling the room temperature strength of reaction sintered silicon nitride, the literature contains no positive direct identification of such defects. Excluding the mechanical damage of surfaces, there appear to be three potential sources of defects:

(a) Porosity developed from the interparticle voids in the original silicon compact, e.g. unfilled or partially filled holes [1–3].

(b) Large silicon particles which are retained (unconverted) in the final material or holes which develop due to the melting of large silicon particles during nitriding [1, 2].

(c) Impurity particles or voids generated due to the presence of impurities [4].

In cases (a) and (b) a close correlation between strength and degree of conversion of the silicon compact would be anticipated as interparticle voids should be progressively filled, or the size of the remaining silicon particles reduced during reaction. Such behaviour is reflected in the linear relationships between strength and nitrided density, and strength and weight gain which have been established for several silicon powders [3, 5]. In cases where the strength is related to the presence of impurity particles, the degree of conversion may be less important than the size, composition and distribution of impurities. Only one of six commercial silicon powders examined at this laboratory has not exhibited a well-defined linear strength/density relationship and subsequent investigation revealed several important factors [6]. Chemical analysis indicated the powder to have an unusually high iron content ($> 1.0\%$) and the measured strengths were extremely variable. Fractographic examination enabled the critical flaws to be identified with ease due to the occurrence of fracture mirrors, and the use of energy dispersive X-ray analysis with the scanning elec-

tron microscope positively identified iron impurities associated with these flaws.

For all other commercial silicon powders [3, 5], however, linear strength/density relationships exist and no such fractographic features are evident: the difficulty of identifying critical defects in reaction sintered silicon nitride by conventional means such as porosimetry, optical or electron microscopy is well known [4, 7, 8]. Measurement of the critical stress intensity factor, K_{IC} of the material provides a means of obtaining the critical surface defect size, $2a$, from the equation [9]:

$$K_{IC} = \sigma Y \sqrt{(2a)} \quad (1)$$

where σ is the stress to propagate the defect and Y is a geometric factor: K_{IC} is related to the critical strain energy release rate, G_c, by the equation

$$G_c = \frac{K_{IC}^2}{E}(1-\nu^2) \quad (2)$$

where E is Young's modulus and ν is Poisson's ratio, and since in a brittle material $G_c = 2\gamma_i$ we can derive the effective surface energy for fracture initiation, γ_i, from a knowledge of K_{IC}, E and ν.

Recent studies [3, 5] have demonstrated that there are linear relationships between strength and nitrided density for most commercial silicon powders which are independent of green density. Consider two green silicon compacts x and y prepared from the same silicon powder but compacted to different green densities ρ_x and ρ_y such that $\rho_x > \rho_y$. If these materials are nitrided to different degrees of conversion such that their nitrided densities are the same, then they will have equivalent strengths [3, 5]. Their structures, however, in terms of the proportions of silicon, silicon nitride and porosity will be very different, but since $\sigma_x = \sigma_y$ and, for a flaw of length $2a$ at the surface

$$\sigma = \frac{1}{Y}\sqrt{\left(\frac{E\gamma_i}{a}\right)} \quad (3)$$

then

$$\frac{E_x\gamma_{ix}}{a_x} = \frac{E_y\gamma_{iy}}{a_y} \quad (4)$$

Because of these structural differences, it was thought unlikely that $E_x = E_y$, $\gamma_{ix} = \gamma_{iy}$, and $a_x = a_y$, so it was concluded that there must be a subtle relationship between these parameters [3].

It has also been demonstrated [10, 11] that nitrogen gas flow during nitriding significantly reduces the strength of the material, although for particular "flow" conditions a strength/density relationship exists.

To investigate why strength/density relationships exist and the influence of gas flow on strength, a series of experiments were designed to nitride silicon compacts of different green densities to varying degrees of conversion under "static" and "flow" conditions. The strength (σ), Young's modulus (E), Poisson's ratio (ν) and critical stress intensity factor (K_{IC}) of these materials were measured and values of the effective surface energy for fracture initiation (γ_i) and critical defect size ($2a$) obtained.

2. Experimental

2.1. Materials and nitriding

A detailed investigation was conducted on a powder known to exhibit a linear strength/density relationship (Table I), which was isostatically pressed at 31 or 185 MN m^{-2} and argon sintered for 4 h at 1175° C to produce low green density (lgd) or high green density (hgd) compacts, respectively. Strength bars 4.57 x 4.57 x 30.00 mm^3, modulus bars 5.00 x 5.00 x 50.00 mm^3 and double torsion plates 25.4 x 25.4 x 2.00 mm^3 (see Section 2.3) were cut from each billet [3]. For each nitriding experiment four strength bars, two modulus bars and four plates from each compact were selected at random and nitrided on silicon nitride trays in a closed end mullite furnace tube at temperatures in the range 1200 to 1350° C. Both "static" and nitrogen "flow" furnace systems were used – full details of the nitriding conditions have been presented elesewhere [10].

TABLE I Characteristics of starting silicon powder

Impurity	(wt %)
Iron	0.87
Aluminium	0.20
Calcium	0.27
Titanium	0.08
Other cations	0.05
Oxygen*	1.0
Median particle size (measured by Coulter counter)	13 μm
Maximum particle size (measured by Coulter counter)	60 μm
Specific surface area (measured by BET)	1.5 m^2 g^{-1}

*Measured by neutron activation analysis.

2.2. Measurement of strength, density and moduli of elasticity

The weights and dimensions of strength and modulus bars were determined before and after nitriding and their densities calculated. Strengths were determined in the as-nitrided condition in three-point bend with a span of 19.05 mm. Rigidity modulus (G), E and ν were determined by the British Ceramic Research Association using established resonant frequency methods [12].

2.3. Determination of K_{IC}

K_{IC} was determined by the double torsion method [13] using a short specimen of the form shown in Fig. 1. It was noted in an earlier investigation [14] that the load to propagate a crack became lower as the crack approached the end of the plate, thus casting some doubt on the values of K_{IC} measured when the crack was in this end region of the sample. In a short specimen of the type used here there is an increased chance that measurements may be made in the region where the end effect occurs and it was therefore necessary to design a testing technique which allowed us to identify and exclude data of this type. Natural cracks were initiated in the specimens at a cross-head speed of 0.05 mm min^{-1} and the load removed. The load required to propagate this crack at the same cross-head speed was then determined, the load being removed as soon as significant crack movement was detected by a drop in load on the recording chart. The load was then reapplied and the procedure repeated so that a number of values (up to 5) for the load to extend the crack were obtained. Only when the first two or three load values for any one specimen were similar was it concluded that the initial crack was far enough from the end of the plate to provide accurate values of K_{IC}. This procedure resulted in the rejection of approximately 25% of the plates tested. When these conditions applied the first load recorded to propagate the crack (P_c) was used to calculate K_{IC} from the equation

$$K_{IC} = P_c W_m \left[\frac{3}{W d^3 d_n (1-\nu)}\right]^{1/2} \quad (5)$$

where W, W_m, d and d_n are the specimen dimensions shown in Fig. 1. Confidence in the K_{IC} data obtained by this procedure was confirmed by testing both 25.4 and 100 mm long plates in both the green and fully nitrided condition when the values obtained from both geometries were in excellent agreement.

3. Moduli of elasticity

E and G are plotted against nitrided density (ρ_n) in Figs. 2 and 3. In each case, separate straight lines fit the data under "static" and "flow" conditions. The equations of these lines and their correlation coefficients (all better than 0.99) are listed in Table II. The E/ρ_n and G/ρ_n relationships are independent of the green density of the compacts, despite the large structural differences which exist at a particular nitrided density between hgd and lgd bars (see Table III).

It is interesting to note that the "static" E/ρ_n

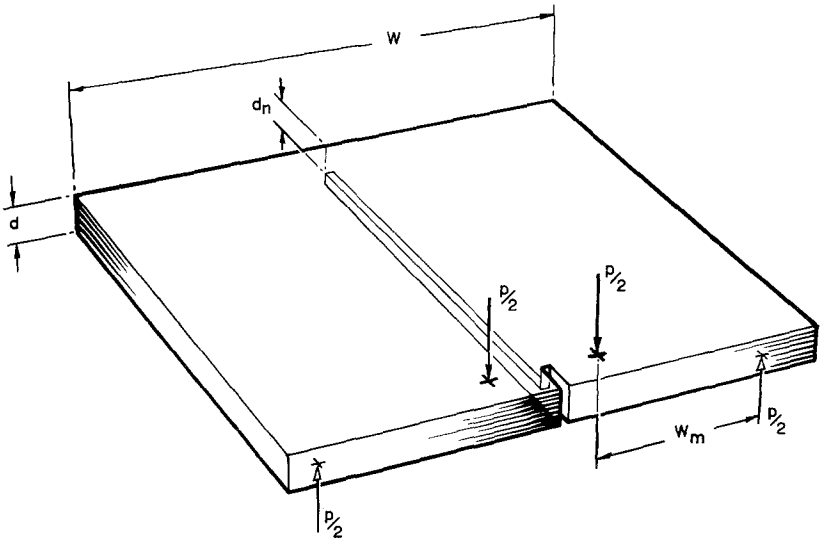

Figure 1 Double torsion specimen.

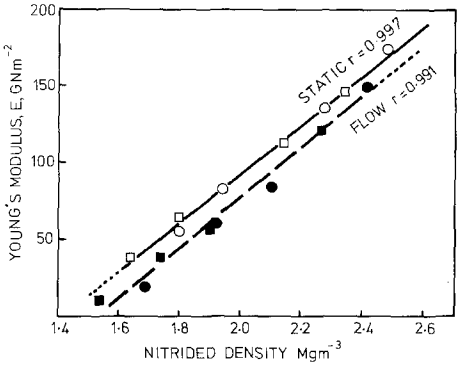

Figure 2 Young's modulus versus nitrided density for lgd and hgd compacts nitrided under "static" and "flow" conditions.

	lgd	hgd	
Static	□	○	——
Flow	■	●	-----

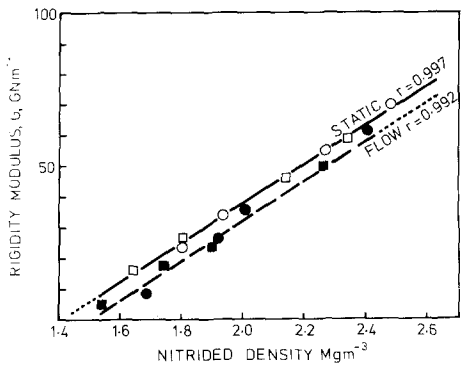

Figure 3 Rigidity modulus versus nitrided density for lgd and hgd compacts nitrided under static and flow conditions. Symbols as in Fig. 2.

line extrapolates to a value of 285 GN m^{-2} at the theoretical density of silicon nitride (3.2 Mg m^{-3}) which is close to the reported value for fully dense silicon nitride (e.g. [1]). The "flow" E/ρ_n line extrapolates to a lower value (272 GN m^{-2}) at theoretical density, but the plotted points suggest that at densities above 2.3 Mg m^{-3} the values for "static" and "flow" tend to converge. The implications of the existence of modulus/density relationships are discussed in Section 7. It is also noted that linear relationships which are dependent on green density exist between elastic moduli and weight gain.

TABLE II Linear equations of Young's modulus, E(GN m^{-2}) versus density, ρ_n(Mg m^{-3}) and rigidity modulus, G(GN m^{-2}) versus density

Nitriding conditions	Equation	Correlation coefficient
Static	$E = 160\,\rho_n - 227$	0.997
	$G = 63.4\,\rho_n - 88.8$	0.997
Flow	$E = 163\,\rho_n - 249$	0.991
	$G = 65.3\,\rho_n - 98.3$	0.992

Values of ν were calculated from the equation

$$\nu = \left(\frac{E}{2G}\right) - 1 \qquad (6)$$

and individual data points are plotted against density in Fig. 4. The separate curves drawn to represent "static" and "flow" data were generated from the appropriate equations for E and G (Table II).

4. Fracture mechanics

4.1. Critical stress intensity factor, K_{IC}

Table IV shows the nitrided densities of the double torsion specimens and the corresponding values of K_{IC} together with values of ν, obtained at appropriate densities from the curves of Fig. 4.

K_{IC} is plotted against nitrided density in Fig. 5. It was not possible to draw separate lines for lgd and hgd materials for either "static" or "flow" specimens, and hence K_{IC} also appears to be independent of green density. A straight line is the most appropriate fit to the "static" data (correlation coefficient 0.936) whilst the curve drawn by eye is obviously a better representation than a straight line for the "flow" data. The values of K_{IC}

TABLE III Comparison of the structure of lgd and hgd compacts after partial nitridation to equivalent densities

Density (Mg m^{-3})	% conversion of silicon to silicon nitride		Relative proportions of phases by volume (%)					
			Silicon nitride		Silicon		Porosity	
	lgd	hgd	lgd	hgd	lgd	hgd	lgd	hgd
1.47 (lgd green)	0	–	0	–	63.1	–	36.9	–
1.60 (hgd green)	–	0	–	0	–	68.7	–	31.3
1.80	33.6	18.8	26.1	15.9	41.9	55.8	32.0	28.3
2.40	94.9	75.1	73.7	63.5	3.2	17.1	23.1	19.4

Volumes of silicon, silicon nitride and porosity have been calculated assuming $\rho_{Si} = 2.33$ Mg m^{-3}, $\rho_{Si_3N_4} = 3.20$ Mg m^{-3}, and that 100% conversion from silicon to silicon nitride represents a weight gain of 66.7%. The lattice volume expansion for silicon to silicon nitride was taken as 23%.

TABLE IV Critical stress intensity factor, K_{IC} for compacts nitrided in "static" and "flow" conditions

Experiment	Compact	Nitrided density ($Mg\,m^{-3}$)	ν	K_{IC} ($MN\,m^{-3/2}$)
Static				
(1) 1 h, 1200° C	lgd	1.65	0.17	0.92
		1.64	0.17	0.83
		1.65	0.17	0.94
		1.64	0.17	0.87
	hgd	1.79	0.20	1.11
		1.77	0.20	0.99
		1.78	0.20	1.11
(2) 5 h, 1200° C	lgd	1.81	0.21	1.11
		1.81	0.21	1.22
	hgd	1.94	0.22	1.26
		1.93	0.22	1.19
		1.93	0.22	1.25
		1.93	0.22	1.28
(3) 5 h, 1300° C	lgd	2.14	0.23	1.41
		2.12	0.23	1.37
		2.16	0.23	1.50
	hgd	2.25	0.23	1.35
		2.25	0.23	1.85
(4) 5 h, 1350° C	lgd	2.34	0.24	1.56
		2.33	0.24	1.71
		2.36	0.24	1.88
	hgd	2.46	0.24	1.74
		2.50	0.24	2.27
		2.48	0.24	1.74
Flow				
(5) 5 h, 1200° C	lgd	1.54	*	0.19
		1.54	*	0.25
		1.54	*	0.28
	hgd	1.69	0.10	0.56
		1.68	0.09	0.46
		1.68	0.09	0.53
(6) 5 h, 1300° C	lgd	1.73	0.12	0.94
		1.76	0.13	0.98
	hgd	1.91	0.18	1.28
		1.90	0.18	1.29
		1.93	0.18	1.37
(7) 5 h, 1330° C	lgd	1.94	0.19	1.37
		1.95	0.19	1.38
		1.91	0.18	1.34
	hgd	2.05	0.20	1.69
		2.15	0.20	1.75
		2.07	0.20	1.61
(8) 20 h, 1330° C	lgd	2.28	0.21	1.79
		2.26	0.21	1.79
		2.31	0.21	1.88
	hgd	2.39	0.22	2.05
		2.40	0.22	2.01

Values of Poisson's ratio (ν) were obtained at the appropriate nitrided density from Fig. 4.
*$\nu = 0$ assumed.

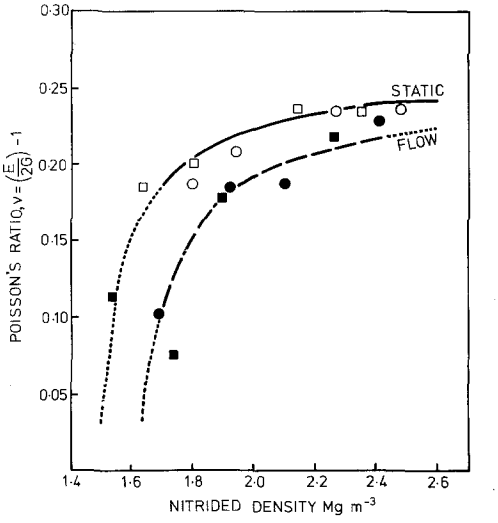

Figure 4 Poisson's ratio versus nitrided density for lgd and hgd compacts nitrided under "static" and "flow" conditions. Smooth curves generated from equations in Table II, symbols as in Fig. 2.

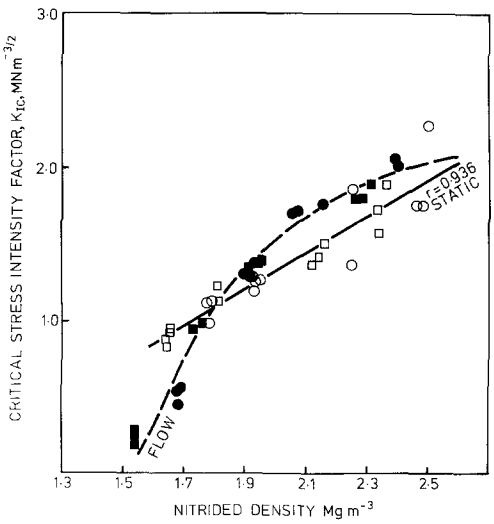

Figure 5 Critical stress intensity factor versus nitrided density for lgd and hgd compacts nitrided under "static" and "flow" conditions. Symbols as in Fig. 2.

for "static" and "flow" are similar over a range of densities from 1.7 to 2.5 Mg m^{-3}. At densities below 1.7 Mg m^{-3}, K_{IC} is lower for "flow" compared to "static" material.

4.2. Effective surface energy for fracture initiation, γ_i

γ_i was calculated for various densities from the equation

$$\gamma_i = \frac{G_c}{2} = \frac{K_{IC}^2(1-\nu^2)}{2E}. \qquad (7)$$

Values of E, ν and K_{IC} were obtained from Figs. 2, 4 and 5. γ_i is plotted against nitrided density for "static" and "flow" data in Fig. 6. Also shown on this graph are the values of γ_i for green hgd and lgd materials. Whilst the values of γ_i for partially and fully nitrided compacts are similar over the density range 1.7 to 2.5 Mg m^{-3}, it is thought that the difference between 9 J m^{-2} for "static" and 15 J m^{-2} for "flow", which occurs at a density of 2.0 Mg m^{-3} is significant. Also of interest is the form of the curves at densities below 1.7 Mg m^{-3} in relation to the values of γ_i for green materials. The trends shown in Fig. 6 suggest that at low densities γ_i "static" increases rapidly to a maximum at a density below 1.7 Mg m^{-3} and then falls as the density increases further. The initial increase of γ_i "flow" with density is more gradual, reaching a maximum at a density of about 2.0 Mg m^{-3} before decreasing again at higher densities.

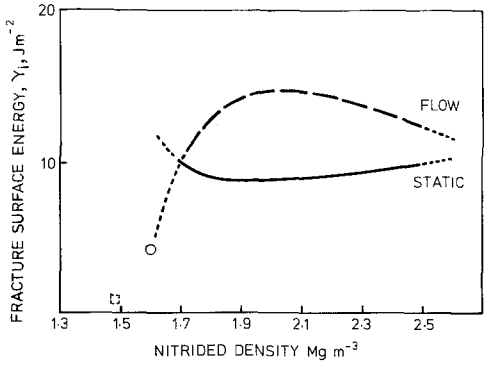

Figure 6 Effective surface energy for fracture initiation versus nitrided density for "static" and "flow" conditions.—— Static, ----- flow, o value measured for green hgd compact, ⬚ value estimated for green lgd compact.

The values of γ_i in the density range 2.3 to 2.5 Mg m^{-3} are 9 to 14 J m^{-2} and correspond closely with the values quoted [1, 15] by workers who have used various fracture mechanics techniques but always natural cracks. Higher values of γ_i (20 to 30 J m^{-2}) are generally reported by investigators who use machined notches (e.g. [16]), and we note that the loads required to initiate a crack from the machined notch in our specimen was, in most cases, significantly larger than the load required to propagate that crack. Thus, contrary to the suggestion in a recent review [17], it appears advisable to use natural cracks for fracture mechanics studies.

TABLE V Critical defect size in green compacts

Material	Density ($Mg\,m^{-3}$)	ν	K_{IC} ($MN\,m^{-3/2}$)	Mean strength ($MN\,m^{-2}$)	Critical defect size (μm)
lgd	1.47	< 0.1	0.14	9	190
hgd	1.60	< 0.1	0.35	14	490

Evans and Davidge [1] reported that γ_i appears, at any particular density to be insensitive to structure in that α/β ratios and the size and distribution of pores have no significant effect. Our observations are in agreement with this but we can extend the statement to include the fact that γ_i is insensitive to the amount of silicon present in the material over a much wider range of structures than those considered by Evans and Davidge. However, our results show that it is necessary to qualify their statement because γ_i is dependent on nitriding conditions as "static" and "flow" values can be different at the same density. Data on a reaction sintered silicon nitride made from a coarser powder and nitrided to complete conversion under "static" conditions indicate a γ_i value of about $7\,J\,m^{-2}$ for a density of $2.5\,Mg\,m^{-3}$. This suggests that γ_i is also dependent upon the properties of the starting silicon powder.

5. Critical defect size, 2a

Using Equations 3 and 7 and assuming that the flaw approximates to a sharp penny-shaped crack over the range of densities studied (e.g. [1, 15, 18]) then

$$Y = \left(\frac{4}{\pi}\right)^{1/2} \tag{8}$$

and the critical defect size was calculated at various densities from

$$2a = \frac{\pi K_{IC}^2 (1-\nu^2)}{4\sigma^2} . \tag{9}$$

At each density values of ν and K_{IC} were obtained from the "static" or "flow" lines of Figs. 4 and 5 respectively. Values of σ were obtained from Fig. 8 and are discussed in Section 6. The curves of critical defect size versus ρ_n for "static" and "flow" conditions are shown in Fig. 7. Confidence in these curves is high for values above $1.7\,Mg\,m^{-3}$. At lower densities the curves are less satisfactory due to uncertainties in the extrapolation of the σ and K_{IC} lines and the rapid change in ν with density. The evidence is conclusive, however, that in the density range 1.7 to $2.6\,Mg\,m^{-3}$, the critical defect size decreases with increasing density for both "static" and "flow" materials. This disagrees with the suggestion [1] that critical defects may result from interparticle voids present in the green silicon compact which do not fill with silicon nitride during conversion. At all densities the critical defect size is larger in "flow" than it is in "static" material and in the density range 2.5 to $2.6\,Mg\,m^{-3}$ the defect size is about $100\,\mu m$ for "flow" and $60\,\mu m$ for "static".

Measurements of critical stress intensity factor, Poisson's ratio and strength were also made on lgd and hgd green silicon compacts and values for the critical defect size calculated from Equation 9 assuming $\nu^2 = 0$. These data are summarized in Table V. The critical defect sizes in this case are extremely large and it is surprising that the defect size for hgd material is larger than that for lgd material. Measurements of the strength of other batches of hgd green silicon compacts have indicated a range of strengths from 8 to $23\,MN\,m^{-2}$. It is suspected, therefore, that the strength of green

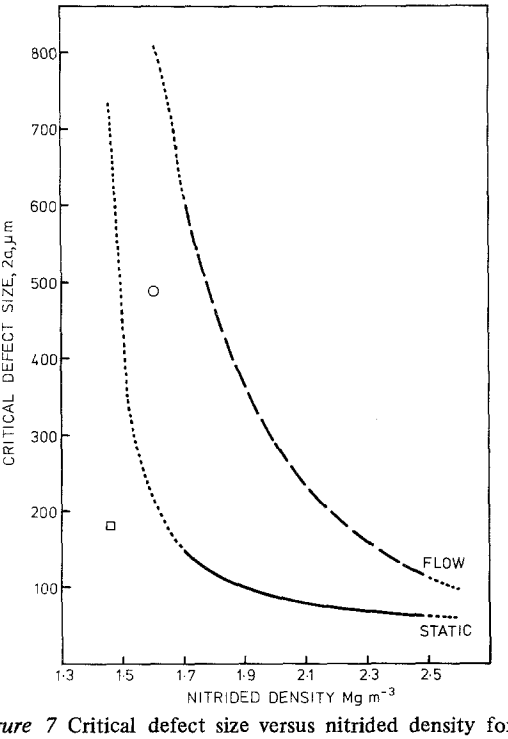

Figure 7 Critical defect size versus nitrided density for "static" and "flow" conditions. ○ value for green hgd material. □ value for green lgd material.

silicon bars is controlled by surface defects which arise in the machining process rather than the interparticle voids in the compact. Despite this, however, it is noted from Fig. 7 that bars nitrided to low weight gains under "flow" conditions contain even larger defects than those which existed in the green silicon bars. The same may be true for lgd bars nitrided under "static" conditions although the uncertainty of the curve below a density of 1.7 $Mg\,m^{-3}$ does not permit a definitive statement. In this particular case there is no evidence to suggest an increase in the defect size for hgd bars nitrided under "static" conditions.

6. Strength

6.1. Observed strength density relationships

Table VI shows values of green density, nitrided density, weight gain and strength for both lgd and hgd compacts nitrided under "static" and "flow" conditions. Mean strength is plotted against nitrided density in Fig. 8 and the separate straight lines fitted to "static" and "flow" data have correlation coefficients of 0.992 and 0.973 respectively. As previously observed [10] for other powders "flow" strengths are significantly lower than "static" strengths.

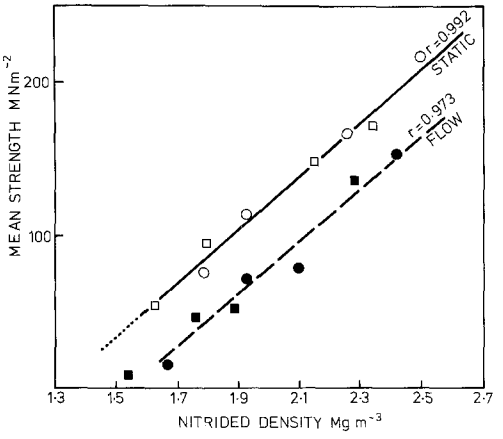

Figure 8 Strength versus nitrided density for lgd and hgd compacts nitrided under "static" and "flow" conditions. Symbols as in Fig. 2.

It is clear from the data reported here that the strength/density relationships are independent of green density because E, γ_i and $2a$ for materials of different green density, nitrided under the same conditions, are identical at any particular nitrided density. The implications of this in terms of the development of the structure of reaction sintered silicon nitride are discussed in Section 7.

TABLE VI Green density, nitrided density, weight gain and strength data for compacts nitrided in "static" and "flow" conditions (all values are means from 4 tests)

Experiment	Compact	Green density ($Mg\,m^{-3}$)	Nitrided density ($Mg\,m^{-3}$)	Weight gain (%)	Mean strength ($MN\,m^{-2}$)
Static					
(1) 1 h, 1200° C	lgd	1.46	1.63	11.9 ± 1.0	55 ± 5
	hgd	1.60	1.78	11.9 ± 0.3	76 ± 2
(2) 5 h, 1200° C	lgd	1.47	1.80	22.8 ± 0.4	95 ± 8
	hgd	1.60	1.93	21.1 ± 0.4	114 ± 9
(3) 5 h, 1300° C	lgd	1.47	2.15	46.6 ± 2.8	148 ± 8
	hgd	1.60	2.26	42.0 ± 1.6	166 ± 15
(4) 5 h, 1350° C	lgd	1.46	2.34	60.0 ± 1.7	171 ± 21
	hgd	1.60	2.50	55.9 ± 1.4	217 ± 7
Flow					
(5) 5 h, 1200° C	lgd	1.47	1.54	4.6 ± 0.3	9 ± 2
	hgd	1.60	1.68	5.2 ± 0.1	15 ± 3
(6) 5 h, 1300° C	lgd	1.47	1.76	19.7 ± 1.7	46 ± 4
	hgd	1.61	1.93	20.5 ± 0.8	71 ± 5
(7) 5 h, 1330° C	lgd	1.46	1.89	29.5 ± 3.1	52 ± 6
	hgd	1.60	2.10	31.4 ± 1.3	79 ± 5
(8) 20 h, 1330° C	lgd	1.48	2.28	54.6 ± 2.7	136 ± 18
	hgd	1.61	2.42	50.3 ± 1.9	153 ± 10

TABLE VII Comparison of the measured strength of green silicon bars with values obtained by extrapolation of the strength/density lines in Fig. 8

Density ($Mg\,m^{-3}$)	Strength ($MN\,m^{-2}$)		
	Measured on green bars	Extrapolated	
		Static	Flow
1.47 (lgd)	8	28	-ve
1.60 (hgd)	14	51	10

6.2. Strength changes at the early stages of nitridation

Table VII compares the experimentally measured values of the strength of lgd and hgd green silicon compacts with values obtained by extrapolating the strength/density lines of Fig. 8 back to the green densities of 1.47 and $1.60\,Mg\,m^{-3}$. Extrapolation of the "static" line gives strengths which are considerably higher than measured values whilst the "flow" line gives a negative strength value at a density of $1.47\,Mg\,m^{-3}$ and a strength of $10\,MN\,m^{-2}$ at a density of $1.60\,Mg\,m^{-3}$. As discussed in Section 5 the low measured strengths of the green bars are attributed to surface flaws formed during machining.

In the case of "flow" the data presented here suggest that strength decreases in the early stages of nitridation. This is supported by other unpublished studies where we have measured strengths less than the green strength in materials nitrided to very low weight gains under both "static" and "flow" conditions. These observations are consistent with an increase in critical defect size during the early stages of the reaction (Section 5).

7. Discussion

7.1. Microstructural model for reaction sintering of silicon compacts

Of the three types of potential critical defect discussed in Section 1, types (b) and (c) are considered unimportant in this material. Melted silicon particles are unlikely since the maximum nitriding temperature was only 1330° C, and unconverted silicon particles (b) do not appear important because their size after nitriding at 1330° C is extremely small. The existence of a good linear relationship between strength and nitrided density, low variability of strength and the absence of fractographic evidence of critical defects are all reasons for eliminating the importance of impurity particles and voids generated due to the presence of impurities as critical defects in the present material.

After consideration of these points and the other data obtained in the present study, a microstructural model for reaction sintered silicon nitride compacts has been formulated.

When the isostatically pressed powders have been sintered in argon, particles are joined by necks of silicon or silica derived from the oxide surface layer present on the original particles. The strengths of bars machined from this material are controlled by either interparticle voids or by larger defects which must result from the breaking of interparticle necks in the regions close to the surface. The evidence suggests that during the early stages of nitridation the interparticle necks are destroyed resulting in a decrease in strength and modulus.

The main evidence for this is:

(i) Strengths lower than the measured green strengths have been recorded for materials nitrided to low weight gains in both "static" and "flow" conditions.

(ii) Young's moduli lower than the measured green Young's moduli have been recorded for materials nitrided to low weight gains under "flow" conditions.

(iii) The evidence of Fig. 7 indicates an increase in the critical defect size during the early stages of nitridation under "flow" conditions and suggests that this can also occur under "static" conditions. Subsidiary evidence is provided by the fact that under the same nitriding conditions the same strength/density relationship is obtained for compacts of a particular powder independent of the critical defect size in the green silicon compact. This point is discussed in detail in Section 7.4.

As the necks between silicon particles are gradually eliminated, silicon nitride begins to form in the void space between silicon particles. The improvement in strength and stiffness following the initial decline must correspond to the development of a continuous skeletal network of whisker-like silicon nitride. It is the densification of this network on further nitridation which gives rise to the linear portions of the strength/density and modulus/density relationships. Once the silicon nitride network has formed, the major voids in the material will be holes which contain the reacting silicon particles. As the reaction proceeds, the silicon particles reduce in size providing additional silicon nitride for the thickening and extension of the silicon nitride network. The mechanism for these processes is in agreement with the theories proposed for the formation of silicon nitride

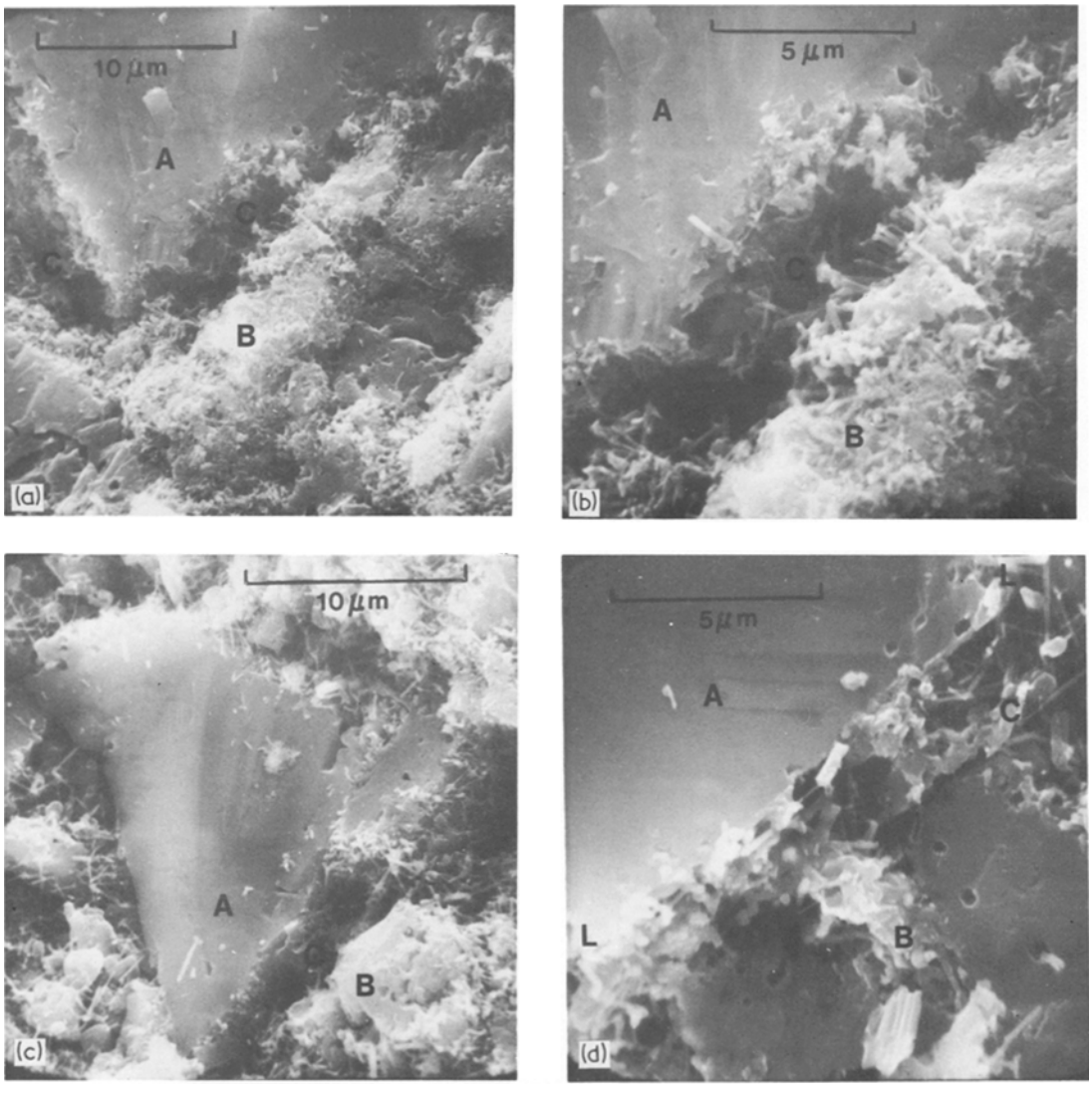

Figure 9 Typical scanning electron micrographs of fracture surfaces of partially nitrided hgd compacts. (a) and (b) Nitrided under "static" conditions to a density of 1.96 $Mg m^{-3}$. Silicon particle is marked A, developing silicon nitride B, and the void space C between these features is noted. The ragged nature of the edge of the silicon particle is evident. (c) and (d) Nitrided under "flow" conditions to a density of 1.92 $Mg m^{-3}$. The smoother nature of the edge of the silicon particle compared to (a) and (b) is obvious and the void space C less clearly defined. A discontinuous surface layer can be seen along the line L-L in (d).

involving vapour-phase transport of silicon monoxide formed from silica and silicon [10, 11, 19, 20]. The mechanism is supported by the microstructural evidence of Fig. 9a and b which shows the interface between a silicon particle and the silicon nitride network to be a gap in a compact converted under "static" conditions. Apart from this evidence, consideration of the mismatch in thermal contraction coefficients of silicon and silicon nitride suggests that it is unlikely that the silicon will contribute to the mechanical properties of the structure at room temperature.

The stage of the process at which the silicon nitride network becomes continuous will depend on both the geometry of the structure (i.e. the size and distribution of the silicon particles and the voids between them) and the proportion of the silicon nitride formed which contributes to the network. The properties of the network at the stage when it becomes continuous will depend on the volume of the silicon nitride contributing to the network and the detailed structure of the network and whisker dimensions. A simplified schematic representation of the early stages of

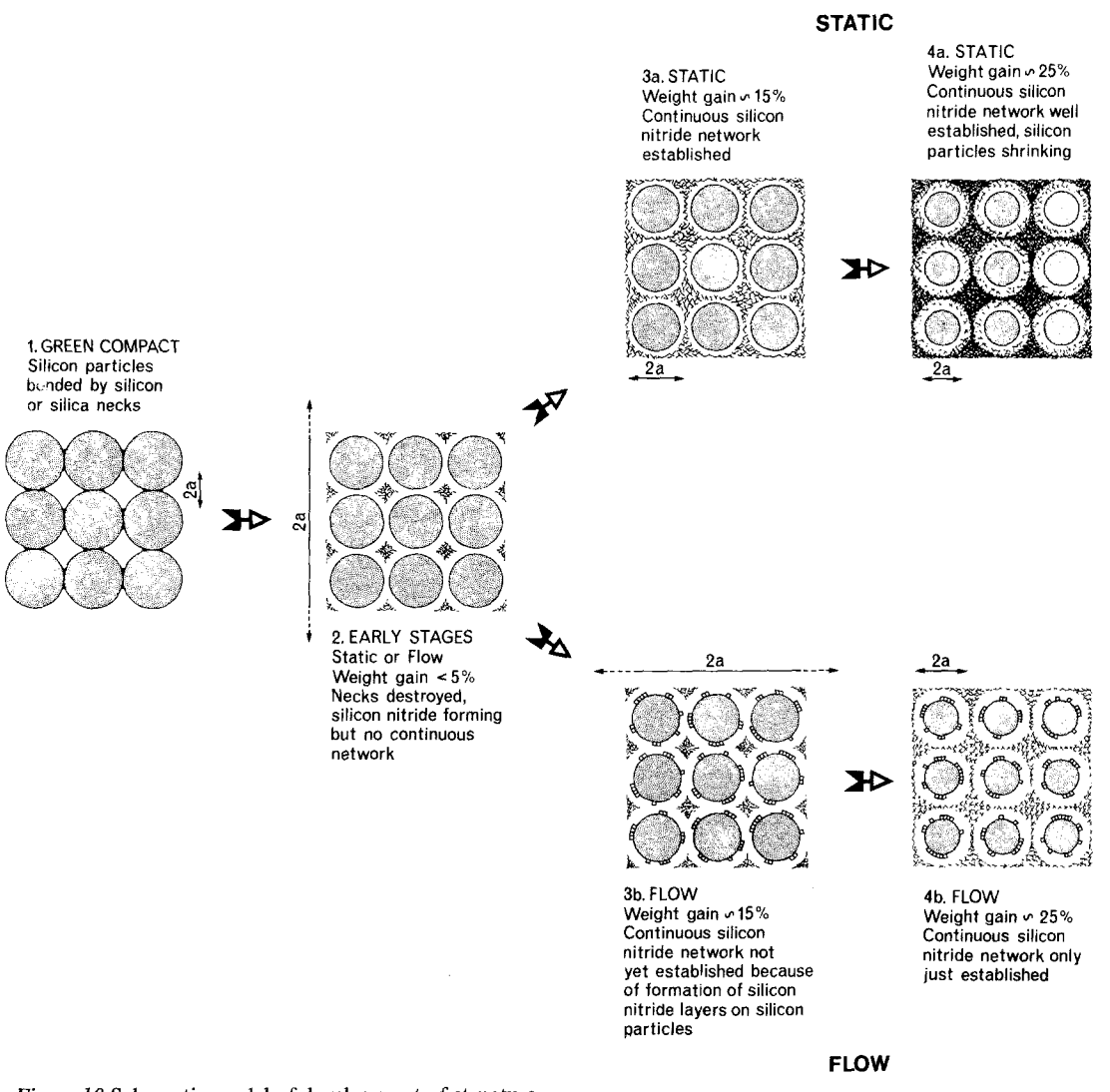

Figure 10 Schematic model of development of structure.

conversion is shown in Fig. 10. The contrast between "static" and "flow" situations is discussed in detail in Section 7.3. The main experimental observations can now be discussed in terms of the proposed mechanism of formation of reaction sintered silicon nitride.

7.2. The existence of strength/density relationships

As noted in Section 6.1 the strength/density relationships are independent of green density because E, γ_i and $2a$ are the same at any particular density despite the fact that low green density material will contain a higher proportion of silicon nitride and less silicon than a material of higher green density (see Table III).

Consider lgd and hgd compacts made from the same silicon powder and nitrided under identical conditions. The particle sizes in the green silicon compacts are identical, but the particles will be further apart and the void spaces larger in lgd compared to hgd compacts. It follows, therefore, that a higher degree of conversion from silicon to silicon nitride will be required to form a continuous network in the more open lgd structure. It must also be remembered that whilst all the silicon nitride formed contributes to the measured density of the material, it will not all contribute to the continuous network, i.e. a proportion of the silicon nitride will be "redundant" as far as mechanical properties are concerned. A higher proportion of the silicon nitride formed in the lgd material will be "redundant" compared to that in hgd material. Whilst a quantitative analysis of this

situation is impossible because the amount of "redundant" silicon nitride is unknown, it seems plausible that the proportion of silicon nitride contributing to the Young's modulus at a given density for lgd and hgd material could be similar, as a result of greater "redundancy" in lgd. It also seems plausible that γ_i and $2a$ could be similar in the two materials as a result of the combination of the geometric relationship of the green structures and the degrees of conversion to silicon nitride required to produce lgd and hgd materials of the same density.

7.3. The effect of "flow"

During the early stages of nitridation the necks which join the silicon particles in the green compacts are gradually eliminated under both "static" and "flow" conditions. This process is likely to be more efficient under "flow" conditions due to the removal of silicon monoxide from the furnace atmosphere in the gas stream [11, 20]. It is difficult to imagine, however, that after elimination of the necks, the silicon particle sizes, spacings or the void spaces are very different for the compacts nitrided under "static" or "flow" conditions (see Fig. 10, stage 2). It is probably the mechanism of network growth which is the most important difference between the two situations (see Fig. 10, stages 3 and 4). It is well established that differences in reaction rate exist between "static" and "flow" systems [10, 20] and the examination of microstructures has indicated the tendency for the formation of surface layers on the silicon particles nitrided in "flow" (Fig. 9c and d) whereas no such layers are observed after "static" nitriding (Fig. 9a and b). Silicon nitride layers of this type have been observed by Atkinson *et al.* [21] and Guthrie and Riley [22] on silicon surfaces nitrided under "flow" conditions. Layers of this nature will not contribute at the early stages to the continuous network of silicon nitride which governs mechanical properties and as such can be considered as part of the "redundant" silicon nitride. Thus for any particular compact the use of "flow" rather than "static" conditions will result in a greater proportion of "redundant" silicon nitride in the structure at any particular nitrided density as illustrated in Fig. 10. This will be reflected in a lower value of Young's modulus and a much larger defect size, and since γ_i is not greatly changed (Fig. 6), a lower strength results.

It follows from this theory that as the silicon nitride network grows and thickens it will absorb into it greater proportions of the silicon nitride which is initially "redundant". In the case of "static" formation this explains why the Young's modulus line extrapolates to a value which corresponds to fully dense silicon nitride at a density of $3.2\,\mathrm{Mg\,m^{-3}}$. Also of interest is the tendency of data points for Young's modulus under "flow" conditions to converge with "static" values, as would be expected as increasing proportions of the "redundant" silicon nitride are absorbed into the continuous network.

7.4. Silicon compact structure

The surface defects which control the strength of green silicon bars must represent a continuous crack path where the necks joining silicon particles are broken. However, if all necks are eliminated at an early stage in the conversion of the compact, the presence of the surface defects will have no significance in terms of the structures which develop around the silicon particles. Thus as long as the surface defect does not significantly alter the geometric arrangement (i.e. crack opening is minimal), regions containing such defects should have the same potential to develop a continuous silicon nitride network as do regions which contain no such defect. This is supported by five pieces of experimental evidence:

(1) In the present experiments much larger defects exist in green hgd bars compared to green lgd bars, yet at densities greater than $1.7\,\mathrm{Mg\,m^{-3}}$ the partially converted materials fall on the same strength/density line and contain critical defects of the same size (Fig. 7).

(2) Different batches of green hgd bars have been prepared from the same powder by the same techniques but exhibit green strengths from 8 to $23\,\mathrm{MN\,m^{-2}}$ implying large differences in the size of surface defects. However, on nitriding, these materials all fall on the same strength/density line (Fig. 8) for specific nitriding conditions.

(3) Batches of a particular silicon powder have been pressed at the same isostatic pressure but sintered in argon or hydrogen at various temperatures up to 1325° C. Minimal densification occurred but green bars machined from these compacts had strengths in the range 8 to $55\,\mathrm{MN\,m^{-2}}$ representing a considerable variation in surface defect size. The strength/density relationships were unchanged despite these differences in initial defect size.

(4) Recent experiments [23] have compared the strengths of as-nitrided bars with those of bars nitrided at the same time but diamond ground and polished to remove 250 μm from the as-nitrided surface. The strengths of diamond ground and polished, and as-nitrided bars were identical at equivalent nitrided densities over a range of weight gains from about 1% up to 60%, suggesting that the strength of the bars is controlled by a surface breaking feature of the bulk microstructure. This information suggests that an incorrect interpretation may have been placed on earlier reported data [7] and agrees with more recent work on the effect of surface finish [4].

(5) Green silicon bars have been fractured in three-point bending so that, although a crack ran through the cross-section of each specimen, the crack opening displacement was minimal and the specimens held together by mechanical keying. Subsequently, these bars have been nitrided and continuous silicon nitride networks were formed, closing the cracks and resulting in the attainment of relatively high strengths for the bars when re-tested in three-point bending.

7.5. The effect of nitriding above the melting point of silicon

It has been noted [1, 2] that the strength of reaction sintered silicon nitride is lower when a large proportion of the nitridation occurs at temperatures above the melting point of silicon. This has been explained [1] in terms of the melting of silicon particles which are bigger than the inter-particle void size producing a new critical defect size in the material and hence reducing strength. The evidence proposed to support such a mechanism [1] appears inconclusive as calculation of the critical defect size from quoted values of E, γ_i and σ reveals that even in the high strength material the defect size may be greater than the maximum particle size and, in the low strength material the defect sizes are almost certainly larger than the maximum particle size. The estimation of pore sizes and their relationship to critical defect sizes by optical microscopy is notoriously difficult, as discussed in Section 1. The explanation based on defects resulting from melted silicon particles cannot apply if reaction sintered silicon nitride forms by the mechanism described in Section 7.1 since the critical defect size is always larger than the silicon particle within it. In terms of the present model, however, a lower strength might be anticipated, if the melted silicon, when subsequently converted to silicon nitride, does not contribute to the continuous network in the same way as silicon nitride formed at temperatures below the melting point.

7.6. Requirements for the production of high strength silicon nitride

The strength of reaction sintered silicon nitride will, in the absence of large impurity particles, be controlled by the structure of the green compact and the conditions under which it is nitrided. It is clear from the arguments presented above that for high strength it is advantageous to produce a green silicon compact with a large number of small voids in close proximity since these can be more efficiently "linked" by the growing silicon nitride network than can relatively few large voids. Small silicon particles will also be advantageous since the critical defect size is obviously "linked" with particle size [5]. Because fine powders are generally more difficult to compact than coarser ones it is likely that the best powder will be one providing an optimum balance between particle size, particle size distribution and compactability. The nitriding conditions which produce the highest strengths are those which will maximize the amount of silicon nitride contributing to the network, the formation of which probably involves vapour transport of the reacting species [11, 19, 20]. Network formation is obviously encouraged by the use of "static" nitriding conditions and by avoiding the melting of silicon particles. It is possible that there are other processing factors which could be adjusted to increase the quantity of silicon nitride which contributes to the continuous network and these are the subject of current research.

8. Conclusions

(1) For a particular silicon powder nitrided under specific conditions, relationships which are independent of green compact density exist between nitrided density and Young's modulus, rigidity modulus, Poisson's ratio, critical stress intensity factor, surface energy for fracture initiation, and critical defect size. The existence of these relationships accounts for the existence of the strength/nitrided density relationship which is independent of green density. The Young's modulus, rigidity modulus and strength/density relationships are linear.

(2) A change in nitriding conditions from

"static" to "flow" changes all the relationships discussed in (1). At any particular density, strengths and moduli are lower and critical defect sizes are considerably greater in "flow" compared to "static" materials.

(3) The experimental observations can be explained in terms of a model which involves the gradual elimination of the necks between silicon particles at an early stage in the nitriding process, followed by the development of a continuous silicon nitride network surrounding the silicon particles. The existence of the strength/density and modulus/density relationships are explained in terms of a greater proportion of "redundant" silicon nitride in low green density compared to high green density compacts. The influence of gas "flow" is to increase the proportion of silicon nitride which does not contribute to the mechanical properties of the continuous network.

Acknowledgements

The authors are indebted to R. L. Brown, B.J. Luxton, W. May and J. Studley for experimental assistance, Mrs. J. Irvine for scanning electron microscopy and to W. R. Davis for modulus measurements. This article is published by permission of the Controller HMSO, holder of Crown Copyright.

References

1. A. G. EVANS and R. W. DAVIDGE, *J. Mater. Sci.* 5 (1970) 314.
2. D. R. MESSIER and P. WONG, Proceedings of the 2nd Army Materials Technology Conference on Ceramics for High Performance Applications, edited by J. J. Burke, A. E. Gorum and R. N. Katz (Brook Hill, Chesnut Hill, Mass, 1974) p. 181.
3. B. F. JONES and M. W. LINDLEY, *J. Mater. Sci.* **10** (1975) 967.
4. D. J. GODFREY, *Proc. Brit. Ceram. Soc.* **25** (1975) 325.
5. B. F. JONES and M. W. LINDLEY, *Powder Met. Int.* 8 (1976) 32.
6. *Idem,* AML data, to be published.
7. D. J. GODFREY and M. W. LINDLEY, *Proc. Brit. Ceram. Soc.* **22** (1973) 229.
8. D. J. GODFREY and K. C. PITMAN in [2], p. 425.
9. P. C. PARIS and G. C. SIH, ASTM Spec. Tech. Publ. No. 381 (1965)
10. B. F. JONES and M. W. LINDLEY, *J. Mater. Sci.* **11** (1976) 1278.
11. D. P. ELIAS and M. W. LINDLEY, *ibid* **11** (1976) 1288.
12. W. R. DAVIS, *Trans. Brit. Ceram. Soc.* **67** (1968) 515.
13. A. G. EVANS, *J. Mater. Sci.* 7 (1972) 1137.
14. K. C. PITMAN, unpublished AML data.
15. B. J. DALGLEISH and P. L. PRATT, *Proc. Brit. Ceram. Soc.* **25** (1975) 295.
16. J. T. BARNBY and R. A. TAYLOR, "Special Ceramics 5" Edited by P. Popper (British Ceramic Research Association, Stoke-on-Trent, 1972) p. 311.
17. J. W. EDINGTON, D. J. ROWCLIFFE and J. L. HENSHALL, *Powder Met. Int.* 7 (1975) 82.
18. R. A. SACK, *Proc. Phys. Soc.* **58** (1946) 729.
19. D. CAMPOS-LORIZ and F. L. RILEY, *J. Mater. Sci.* **11** (1976) 195.
20. D. P. ELIAS, B. F. JONES and M. W. LINDLEY, *Powder Met. Int.* 8 (1976) 162.
21. A. ATKINSON, A. J. MOULSON and E. W. ROBERTS, *J. Mater. Sci.* **10** (1975) 1242.
22. R. B. GUTHRIE and F. L. RILEY, *Proc. Brit. Ceram. Soc.* **22** (1973) 275.
23. B. F. JONES and M. W. LINDLEY, AML data, to be published.

Received 22 April and accepted 2 July 1976.